Optical Frequency Standards Based on the $^{199}Hg^+$ Ion

U. Tanaka, J. C. Bergquist, S. Bize, S. A. Diddams, R. E. Drullinger, L. Hollberg, W. M. Itano, C. E. Tanner, and D. J. Wineland

***Abstract*—We report on work directed toward the systematic evaluation of an optical frequency standard based on the $^2S_{1/2}$-$^2D_{5/2}$ transition of a single, laser-cooled, trapped $^{199}Hg^+$ ion, whose resonance frequency is 1.06 $\times 10^{15}$ Hz. For the purpose of the evaluation, a second $^{199}Hg^+$ standard has been constructed. In the cooling-laser system built for the second standard, an injection-locking scheme has been applied to a CW Ti-sapphire laser. We also report optical frequency measurements of the clock transition performed over the past 21 months with the first standard. During this term, the variation of the clock transition frequency is found to be less than $\pm 1 \times 10^{-14}$.**

***Index Terms*—Injection-locked laser, mercury ion, optical frequency standard.**

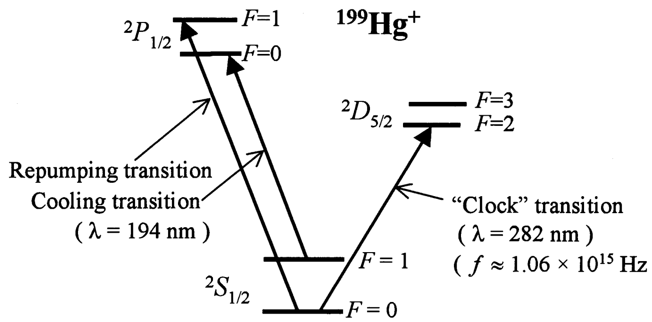

Fig. 1. Partial energy level diagram for $^{199}Hg^+$.

I. Introduction

An OPTICAL clock based on a single trapped ion promises higher stability and accuracy than those of present-day time standards. Significant recent developments have made an optical clock more feasible. First, the realization of sub-hertz linewidth laser systems [1], [2] and the development of mode-locked femtosecond lasers as coherent frequency-comb generators [3]–[5] have now made possible accurate measurements of absolute optical atomic frequencies [6], [7]. Second, an all-optical atomic clock comprising a femtosecond comb that is referenced to a narrow transition in a single trapped $^{199}Hg^+$ ion has been demonstrated. A fractional frequency instability (Allan deviation) of 7×10^{-15} at 1 s was obtained for this clock [8]. The quantum-limited instability of a laser locked to the Hg^+ ion is expected to be about $1 \times 10^{-15}\tau^{-1/2}$, where τ is the measurement period in seconds, with a fractional frequency uncertainty approaching 10^{-18}[9], [10]. To achieve this goal, experimental evaluations of the uncertainty, which can be made by comparing two independent systems, are indispensable.

In this paper, we report our progress in the development of a second Hg^+ ion frequency standard built for the purpose of a systematic evaluation of the first frequency standard. In particular, we describe a second light system for laser cooling that uses a CW injection-locked Ti-sapphire laser. We also report optical-frequency measurements of the clock transition of the $^{199}Hg^+$ ion, of which measurements have been performed over the past 21 months. During this period, the variation of the clock transition frequency was found to be less than $\pm 1 \times 10^{-14}$.

Manuscript received June 17, 2002; revised November 12, 2002. This work was supported in part by the Office of Naval Research. The work of U. Tanaka was supported by the former Science and Technology Agency of Japan (presently Ministry of Education, Culture, Sports, Science and Technology).

U. Tanaka is with the Communications Research Laboratory, Kobe 651-2492 Japan.

J. C. Bergquist, S. A. Diddams, R. E. Drullinger, L. Hollberg, W. M. Itano, and D. J. Wineland are with the National Institute of Standards and Technology, Boulder, CO 80305 USA.

S. Bize is with the Laboratoire Systèmes de Référence Temps-Espace, 75014 Paris, France.

C. E. Tanner is with the Department of Physics, University of Notre Dame, Notre Dame, IN 46556-5670 USA.

Digital Object Identifier 10.1109/TIM.2003.810008

II. Atomic System and Experimental Setup

A partial energy-level diagram of $^{199}Hg^+$ is shown in Fig. 1. The $^2S_{1/2}(F=0, M_F=0)$-$^2D_{5/2}(F=2, M_F=0)$ electric-quadrupole transition at 282 nm provides the reference for the optical standard. The natural linewidth of the S-D transition is about 2 Hz at a resonance frequency of 1.06×10^{15} Hz. The 282 nm radiation used to drive the clock transition is generated in a nonlinear crystal as the second harmonic of a dye laser oscillating at 563 nm. A laser linewidth below 0.2 Hz for averaging periods from 1 to 10 s is realized by locking the frequency of the dye laser to a high-finesse Fabry–Pérot cavity that is temperature-controlled and supported on an isolation platform [1]. The $^2S_{1/2}(F=1)$-$^2P_{1/2}(F=0)$ transition at 194 nm is used for laser cooling. Another 194-nm light beam (the repumper) tuned to the $^2S_{1/2}(F=0)$–$^2P_{1/2}(F=1)$ transition is employed to return the ion to the ground state $F=1$ level. These transitions are also used for state preparation and detection.

A single, laser-cooled $^{199}Hg^+$ ion is confined in a cryogenic, spherical Paul trap. Under typical operating conditions, the radial secular frequency of the trapped ion is between 1.2 and 1.5 MHz. Static-potential biasing electrodes are mounted near the trap electrodes, but outside the trapping volume, to cancel stray static-electric fields at the site of the ion. The trap electrodes are housed in a vacuum system held at liquid-helium temperature. At room temperature, collisions with background neutral mercury and hydrogen occasionally result in the formation of either Hg_2^+ or HgH^+ and the loss of the single Hg^+. Use of a cryogenic system prevents this loss and has made it possible to confine a single $^{199}Hg^+$ ion continuously for more than 100 days.

Transitions to the D state were detected using the technique of "electron shelving" [11], [12], which infers the presence of the atom in the metastable level through the absence of scattering from the strong laser transition at 194 nm [9]. Laser-cooling, state preparation, excitation of the clock transition, and subsequent detection comprise one measurement cycle. After the ion was laser-cooled to near the Doppler limit of 1.7 mK, the ion was prepared in the $^2S_{1/2}(F = 0, M_F = 0)$ state by blocking the repumping laser. Following this, the cooling laser was also blocked, and in the absence of any 194-nm radiation, the ion was irradiated by the 282-nm light for a period between 10 and 120 ms. Finally, the 194-nm lasers were re-applied and the presence or absence of scattered light was used to determine whether the clock transition occurred. The next cycle commences when the ion is again in the ground state (determined by the presence of scattered light at 194 nm). The linewidths of the observed resonance are limited by the probe time of the 282-nm light. When the clock transition was probed for a period of 120 ms, a linewidth of 6.5 Hz was obtained [9]. For the purpose of locking the frequency of the laser to the clock transition of the single ion, the duration of the 282-nm light was set typically between 20 and 40 ms, which gave a linewidth of approximately 40 to 20 Hz, respectively. Usually, 48 measurements were made on each side of the resonance before correcting the frequency of the laser toward line center.

III. Second Hg^+ Optical Frequency Standard

In order to aid in the evaluation of the systematic shifts and their uncertainties, we built a second mercury optical frequency standard comprising a second cryogenic Hg^+ trap and a second 194-nm light source. Narrow-band 563-nm radiation is provided to both systems from the same light source. The frequency of the 563-nm radiation is independently doubled and shifted into resonance with the clock transition of each standard by means of acoustooptic modulators.

Fig. 2 shows a schematic diagram of the second 194-nm light source. The 194 nm radiation is produced by sum-frequency generation with a beta-barium borate (BBO) crystal, where the wavelengths of the fundamental beams are 257 and 792 nm [13]. The power of both light sources at 792 nm is enhanced in a resonant cavity, while the 257-nm light is single passed through the BBO. The power enhancement cavity at 792 nm is locked to resonance with the radiation source at 792 nm that is used to sum-frequency generate the 194-nm light used for Doppler cooling. The 194-nm beam used as the repumper is also generated in the same BBO crystal by phase-offset locking a second extended-cavity diode laser to the primary 792-nm source such that it is simultaneously resonant with the $^2S_{1/2}(F = 0)$-$^2P_{1/2}(F = 1)$ transition and with a second axial mode of the cavity. The 257-nm radiation is generated by frequency-doubling the 515-nm light from a single-frequency argon-ion laser and is similar to that described in [13].

The frequency of the 515-nm light is locked to a hyperfine component of molecular iodine by feedback to a piezo-mounted

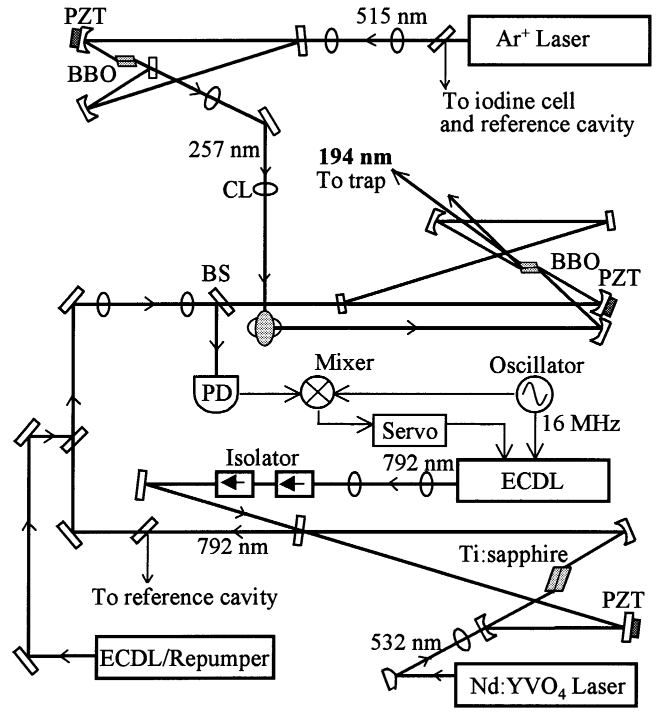

Fig. 2. Schematic diagram of the second 194-nm light source for the cooling transition. ECDL: extended cavity diode laser; PD: photodetector; PZT: piezoelectric transducer; CL: cylindrical lens; BS: beam splitter.

cavity mirror. Some of the output power of the stabilized argon ion laser is guided into a confocal Fabry–Pérot cavity that is 10 cm long and whose mirrors are coated for both 515 and 792 nm. The long-term drift of this cavity is reduced by locking it to the stable 515-nm source. When the frequency of the 792-nm source is then locked to a fringe of the cavity, the stability of the argon-ion laser is transferred to the 792-nm laser and thereby to the 194-nm radiation.

The main difference between the two 194-nm sources is that the 792-nm radiation in the second system is produced by an injection-locked Ti-sapphire laser [14]. This choice was primarily dictated by experimental convenience given available equipment, but it nonetheless forms an interesting laser. This method requires only simple optics in the Ti-sapphire laser cavity (the four cavity mirrors plus Ti-sapphire crystal).

The master laser at 792 nm is an extended-cavity diode laser in the Littman configuration. The power of the zeroth-order reflection beam is 11 mW, and the continuous scanning range is about 2 GHz. This beam is mode-matched to the Ti-sapphire cavity with two lenses followed by two successive isolators that give an isolation greater than 60 dB. Because of losses through the isolators, only about 8 mW of power from the master laser reaches the Ti-sapphire cavity.

The Ti-sapphire cavity consists of a 10-mm-long, Brewster-cut Ti-sapphire crystal, two mirrors with a common radius of curvature of 15 cm, a flat mirror, and a flat output coupler with a reflectivity of 97.6%. All of the other mirrors have a reflectivity exceeding 99.9%. The round-trip length is 157 cm and the minimum beam waist, located in the Ti-sapphire crystal, is 33 μm. No other optical element is necessary since the master laser forces single-frequency and unidirectional

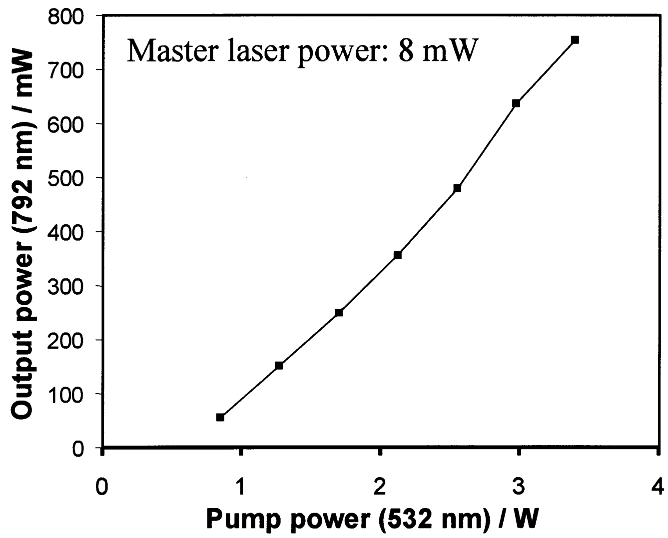

Fig. 3. Output power of the injection-locked Ti-sapphire laser. The pump power is corrected for the transmission of the 532-nm light through the cavity mirror, which is highly reflecting at 792 nm.

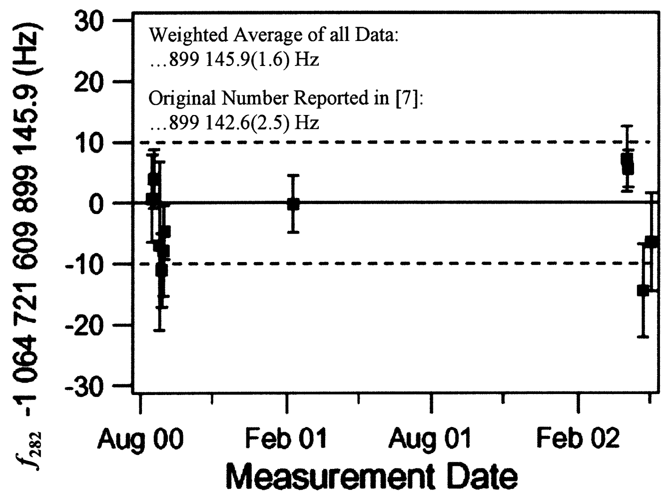

Fig. 4. A chronological record of the average daily frequency of the clock transition measured since August 2000. The dotted lines indicate the 10-Hz systematic uncertainty of the optical frequency measurements.

operation. A commercial, frequency-doubled Nd:YVO$_4$ laser at 532 nm is used as the pump laser.

As in [14], the frequency of the extended-cavity diode laser is locked to the resonance of the Ti-sapphire cavity by the Pound–Drever–Hall technique [15]. The current of the diode laser is modulated at 16 MHz. A beam splitter is inserted in the Ti-sapphire laser beam such that 0.5% of the power is monitored with a photodetector. The ac component of the monitored signal is demodulated and used as the error signal. The feedback circuit consists of a fast and slow loop. The fast component of the error signal controls the master laser current and the slow component is used to correct the cavity length of the master laser. When free-running, the resonance of the Ti-sapphire laser cavity is driven by acoustical noise and fluctuates about 20 MHz. We reduce this jitter by locking the frequency of the Ti-sapphire laser to the reference cavity that is stabilized to the argon-ion laser. With the servo loop closed, the jitter can be reduced below 1 MHz.

Fig. 3 shows the output power of the injection-locked Ti-sapphire laser as a function of pump power for a constant master-laser power of 8 mW. The output power is measured following the beam splitter used to derive the error signal. At pump powers higher than 3 W, the injection lock becomes unstable. The locking range has been shown to depend on the ratio between the power of the master laser and that of the slave laser [14], [16]. Either by using a master laser with more power or by better coupling of the master laser into the Ti-sapphire cavity, we could make the injection-locked laser stable at higher pump powers [14], [16].

A power-enhancement cavity for the 792-nm radiation is used for the sum-frequency generation of the 194-nm radiation. The 792-nm enhancement cavity is formed by two 10-cm radius–of-curvature mirrors and two flat mirrors. The round-trip length of the cavity is 72.5 cm, and the minimum cavity waist size is approximately 31 μm. A 3 mm $\times$ 3 mm $\times$ 6 mm, Brewster-cut and angle-tuned BBO crystal is placed at this waist. For this configuration, we can obtain a power-enhancement factor of about 110. The cavity length is locked to the frequency of the 792-nm source by use of the Hänsch–Couillaud method [17]. The 257-nm beam is focused through the BBO crystal with a highly reflective mirror that has a radius of curvature of 10 cm. The incident angle is adjusted so that both fundamental beams are collinear inside the crystal. With 14 mW of power at 257 nm and 400 mW of power at 792 nm, 48 μW of output power at 194 nm is obtained. For the Hg$^+$ experiments, we operate with a power of about 25 μW in order to avoid saturation of the $^2S_{1/2}(F=1)$-$^2P_{1/2}(F=0)$ transition.

Finally, a second, cryogenic, ion-trap system, which has the same dimensions as the first standard [7], has been constructed. So far, single ions have been loaded and laser-cooled. Work is now directed toward locking the frequency of the clock laser to the S–D transition in the second system and comparing its frequency to that of the first Hg$^+$ standard.

IV. Frequency Measurements of the Clock Transition

Optical frequency measurements of the clock transition are made by use of an optical frequency comb [3]–[7]. The 563-nm light is transferred to the comb through an optical fiber. If we choose the nth mode of the comb whose frequency is lower than the fundamental laser frequency f_{563}, the laser frequency is given by $f_{563} = f_0 + nf_r + f_b$, where f_0 is the frequency offset common to all modes of the comb, f_r is the repetition frequency of the comb (which is about 1 GHz), and f_b is a beat frequency between f_{563} and the nth mode of the comb. The offset frequency f_0 and the beat frequency f_b are locked to a hydrogen maser by controlling the pump power and the cavity length of the mode-locked femtosecond laser, respectively. To obtain the value of f_{563}, we count f_r with a high-resolution counter that is also referenced to the hydrogen maser. The frequency of the maser [18] is calibrated by comparing it to the local NIST primary standard NIST-F1 [19]. The fractional uncertainty in the frequency of the reference maser reaches 1.8×10^{-15} for these measurements.

Fig. 4 summarizes the frequency measurements of Hg$^+$ made between August 2000 and May 2002. The second-order Zeeman shift was corrected for all values. The statistical uncertainty of the frequency measurements is limited by the fractional frequency instability of the reference maser, which reaches about 1.6×10^{-15} in our measurement time of 20 000 s. The weighted mean of our measurements of the Hg^+ clock transition is $f_{282} = 1\,064\,721\,609\,899\,145.9(1.6)(10)$ Hz, where 1.6 Hz is the statistical uncertainty and 10 Hz is the conservative estimate of the systematic uncertainty.

It should be possible to reduce the uncertainties of all systematic shifts to values approaching 10^{-18}[10]. The ${}^2S_{1/2}(F=0, M_F=0)$-${}^2D_{5/2}(F=2, M_F=0)$ transition has no linear Zeeman shift, but it does have a quadratic Zeeman shift, a second-order Stark shift (such as the shift due to the blackbody radiation), and a shift due to the interaction between the electric-field gradient and the atomic electric-quadrupole moment. None of these shifts has yet been measured accurately but their values have recently been calculated by one of us [10]. The largest uncertainty is expected to arise from the quadrupole shift, which is caused by the interaction between the atomic quadrupole-moment of the ${}^2D_{5/2}$ state and a static electric field gradient. In spherical Paul traps, no static field gradient is deliberately applied; however, a gradient can exist due to patch potentials that are randomly distributed on the trap electrodes. For example, in our trap, a static potential of 1 V between ring and endcaps could give a quadrupole shift as large as 1 Hz [10]. This shift can be eliminated by averaging the S–D transition frequency over three mutually orthogonal, equal-magnitude magnetic field orientations [10].

V. Conclusion

We have measured the optical clock transition of the ${}^{199}Hg^+$ ion on several occasions spanning more than 21 months. The weighted average frequency for these measurements is $f_{282} = 1\,064\,721\,609\,899\,145.9(1.6)(10)$ Hz. We anticipate that the largest uncertainty in the clock transition frequency is due to the atomic quadrupole shift, which is dependent on the orientation of the applied magnetic field, and which we have not corrected so far. To assist in the evaluation of the systematic uncertainty experimentally, we have built a second Hg^+ standard. We have applied an injection-locking scheme to generate high-power 792-nm radiation as one of the fundamental sources used in sum-frequency generation of 194-nm light. With 400 mW of 792-nm light enhanced in a cavity and 14 mW of 257-nm light, 48 μW of the 194-nm radiation is obtained.

Acknowledgment

The authors are grateful to T. Parker, S. Jefferts, and T. Heavner for providing the absolute frequency calibration and to A. Bartels of Giga-Optics GmbH for his valuable assistance with the femtosecond laser. They also thank R. Windeler of Lucent Technologies for providing the microstructure optical fiber.

References

[1] B. C. Young, F. C. Cruz, W. M. Itano, and J. C. Bergquist, "Visible lasers with subhertz linewidths," *Phys. Rev. Lett.*, vol. 82, pp. 3799–3802, 1999.
[2] J. C. Bergquist, R. J. Rafac, B. C. Young, J. A. Beall, W. M. Itano, and D. J. Wineland, "Sub-dekahertz spectroscopy of ${}^{199}Hg^+$," in *Proc. SPIE*, vol. 4269, 2001, pp. 1–7.
[3] T. Udem, J. Reichert, R. Holzwarth, and T. W. Hansch, "Absolute optical frequency measurement of the cesium D_1 line with a mode-locked laser," *Phys. Rev. Lett.*, vol. 82, pp. 3568–3571, 1999.
[4] S. A. Diddams, D. J. Jones, J. Ye, S. T. Cundiff, J. L. Hall, J. K. Ranka, R. S. Windeler, R. Holzwarth, T. Udem, and T. W. Hansch, "Direct link between microwave and optical frequencies with a 300 THz femtosecond laser comb," *Phys. Rev. Lett.*, vol. 84, pp. 5102–5105, 2000.
[5] D. J. Jones, S. A. Diddams, J. K. Ranka, A. Stentz, R. S. Windeler, J. L. Hall, and S. T. Cundiff, "Carrier-Envelope phase control of femtosecond mode-locked lasers and direct optical frequency synthesis," *Science*, vol. 288, pp. 635–639, 2000.
[6] K. R. Vogel, S. A. Diddams, C. W. Oates, E. A. Curtis, R. J. Rafac, W. M. Itano, J. C. Bergquist, R. W. Fox, W. D. Lee, J. S. Wells, and L. Hollberg, "Direct comparison between two cold-atom-based optical frequency standards using a femtosecond-laser comb," *Opt. Lett.*, vol. 26, pp. 102–104, 2001.
[7] T. Udem, S. A. Diddams, K. R. Vogel, C. W. Oates, E. A. Curtis, W. D. Lee, W. M. Itano, R. E. Drullinger, J. C. Bergquist, and L. Hollberg, "Absolute frequency measurements of the Hg^+ and Ca optical clock transitions with a femtosecond laser," *Phys. Rev. Lett.*, vol. 86, pp. 4996–4999, 2001.
[8] S. A. Diddams, T. Udem, J. C. Bergquist, E. A. Curtis, R. E. Drullinger, L. Hollberg, W. M. Itano, W. D. Lee, C. W. Oates, K. R. Vogel, and D. J. Wineland, "An optical clock based on a single trapped ${}^{199}Hg^+$ ion," *Science*, vol. 293, pp. 825–828, 2001.
[9] R. J. Rafac, B. C. Young, J. A. Beall, W. M. Itano, D. J. Wineland, and J. C. Bergquist, "Sub-dekahertz ultraviolet spectroscopy of ${}^{199}Hg^+$," *Phys. Rev. Lett.*, vol. 85, pp. 2462–2465, 2000.
[10] W. M. Itano, "External-field shifts of the ${}^{199}Hg^+$ optical frequency standard," *J. Res. Nat. Inst. Stand. Technol.*, vol. 105, pp. 829–837, 2000.
[11] H. G. Dehmelt, "Proposed $10^{14}\Delta v < v$ laser fluorescence spectroscopy on Tl^+ mono-ion oscillator II," *Bull. Amer. Phys. Soc.*, vol. 20, p. 60, 1975.
[12] J. C. Bergquist, W. M. Itano, and D. J. Wineland, "Recoilless optical absorption and Doppler sidebands of a single trapped ion," *Phys. Rev. A*, vol. 36, pp. 428–430, 1987.
[13] D. J. Berkeland, F. C. Cruz, and J. C. Bergquist, "Sum-frequency generation of continuous-wave light at 194 nm," *Appl. Opt.*, vol. 36, pp. 4159–4162, 1997.
[14] E. A. Cummings, M. S. Hicken, and S. D. Bergeson. A 1 W injection locked cw titanium:sapphire laser. [Online]. Available: http://arXive.org/abs/physics/0 112 014
[15] R. W. P. Drever, J. L. Hall, F. B. Kowalski, J. Hough, G. M. Ford, A. J. Munley, and H. Ward, "Laser phase and frequency stabilization using an optical resonator," *Appl. Phys. B*, vol. 31, pp. 97–105, 1983.
[16] A. E. Siegman, *Lasers*. Mill Valley, CA: University Science, 1986, pp. 1129–1170.
[17] T. W. Hänsch and B. Couillaud, "Laser frequency stabilization by polarization spectroscopy of a reflecting reference cavity," *Opt. Commun.*, vol. 35, pp. 441–444, 1980.
[18] T. E. Parker, "Hydrogen maser ensemble performance and characterization of frequency standards," *Proc. 1999 Joint Meeting of the Eur. Frequency and Time Forum and the IEEE Int. Frequency Control Symp.*, pp. 173–176, 1999.
[19] S. R. Jefferts, J. Shirley, T. E. Parker, T. P. Heavner, D. M. Meekhof, C. Nelson, F. Levi, G. Costanzo, A. DeMarchi, R. Drullinger, L. Hollberg, W. D. Lee, and F. L. Walls, "Accuracy evaluation of NIST-F1," Metrologia, vol. 39, no. 5, 2002, to be published.

U. Tanaka, photograph and biography not available at the time of publication.

J. C. Bergquist, photograph and biography not available at the time of publication.

S. Bize, photograph and biography not available at the time of publication.

S. A. Diddams, photograph and biography not available at the time of publication.

R. E. Drullinger, photograph and biography not available at the time of publication.

L. Hollberg, photograph and biography not available at the time of publication.

W. M. Itano, photograph and biography not available at the time of publication.

C. E. Tanner, photograph and biography not available at the time of publication.

D. J. Wineland, photograph and biography not available at the time of publication.